

MECHANICAL

TECHNOLOGY

INCORPORATED

GPO PRICE \$ \_\_\_\_\_

CFSTI PRICE(S) \$ \_\_\_\_\_

Hard copy (HC) 5.00

Microfiche (MF) 1.50

# 653 July 65

N66 28483

(ACCESSION NUMBER)

42

(PAGES)

CR-75696

(NASA CR OR TMX OR AD NUMBER)

(THRU)

1

(CODE)

14

(CATEGORY)

CR-75696

MECHANICAL TECHNOLOGY INCORPORATED  
968 Albany-Shaker Road  
Latham, New York

MTI-65TR63

INVESTIGATION OF AN AXIAL-EXCURSION  
TRANSDUCER FOR SQUEEZE-FILM BEARINGS

by

F.K. Orcutt  
C. Kissinger  
C.H.T. Pan

Contract No. NAS8-11678

December, 1965

TECHNICAL REPORT  
INVESTIGATION OF AN AXIAL-EXCURSION  
TRANSDUCER FOR SQUEEZE-FILM BEARINGS

by  
F.K. Orcutt  
C. Kissinger  
C.H.T. Pan

*F.K. Orcutt C. Kissinger C.H.T. Pan*

Author (s)

*Ben Sternlicht*

Approved

Approved

Prepared for

NATIONAL AERONAUTICS AND SPACE ADMINISTRATION  
GEORGE C. MARSHALL SPACE FLIGHT CENTER

Prepared under

Contract No. NAS8-11678

**MTI**  
MECHANICAL TECHNOLOGY INCORPORATED  
**MTI**

968 ALBANY - SHAKER ROAD — LATHAM, NEW YORK — PHONE 785-0922

## TABLE OF CONTENTS

	<u>page</u>
I. INTRODUCTION . . . . .	1
II. SUMMARY OF AXIAL-EXCURSION TRANSDUCER PERFORMANCE . . . . .	3
III. EXPERIMENTAL AXIAL-EXCURSION SQUEEZE-FILM TRANSDUCER APPARATUS .	5
IV. EXPERIMENTAL OPERATION OF THE AXIAL-EXCURSION TRANSDUCER . . . .	8
A. Survey of Transducer Resonant Frequencies . . . . .	8
B. Characteristic Bearing Cone Motion . . . . .	9
C. Effect of Drive Voltage . . . . .	13
D. Effect of Preload . . . . .	14
E. Effects of Bearing Mass . . . . .	15
F. Effect of Clamping Ring Mass . . . . .	16
G. Effect of Centerplane Mounting Ring . . . . .	17
V. CONCLUSIONS AND RECOMMENDATIONS . . . . .	19
LIST OF REFERENCES . . . . .	22
FIGURES	

## 1. INTRODUCTION

In a squeeze film gas bearing, the bearing surfaces are vibrated relative to one another in the plane normal to the surfaces. If the vibration frequency is high, during each cycle of oscillation gas in the space between the bearing surfaces is alternately compressed and expanded. Because of non-linear effects, the integrated pressure in the bearing film over a full cycle of oscillation is greater than the ambient pressure. For this reason, the squeeze-film bearing is able to sustain a load. The purpose of the phase of the squeeze-film gyro bearing program covered by this report is to evaluate and perform preliminary development work on advanced concepts for the transducer system which provides the high-frequency vibratory motion of the bearing surfaces.

For a given bearing surface geometry and mean gap between surfaces, the bearing load capacity and stiffness increase with increased vibration amplitude. Or, stated another way, specified bearing load capacity and stiffness can be achieved with a larger mean gap if the vibratory motion amplitude is increased. Vibratory motion of the bearing surfaces can be achieved through piezoelectric, magnetostrictive or electro-magnetic drivers. Piezoelectric transducers are preferred over the others because they offer the best combination of high driving frequencies, large vibratory amplitudes, low power dissipation and low weight. However, the piezoelectric transducers which have so far been used in squeeze-film bearing systems have given bearing surface vibrations amplitudes of only about  $10^{-4}$  in. peak-to-peak per inch of bearing diameter. Larger vibration amplitudes result in dangerously high stresses in the piezoelectric material and very rapidly rising power dissipation. These small vibration amplitudes mean very small mean bearing gaps (on the order of  $10^{-4}$  in./in. for optimum performance). If the vibration amplitude can be increased appreciably, a proportionate increase in the mean

bearing gap can be made with no loss in performance. One way of doing this without large piezoelectric material stresses and with low power loss is to connect the bearing to the driving transducer through a mechanical flexure so the transducer motion is amplified at the bearing surface by deflection of the flexure.

The experimental axial-excursion transducer system with flexure support of the bearings is shown schematically in Fig. 1. Conical bearings at each end of the transducer support and locate the gyro float (not shown) in both the radial and the axial planes. The tubular, ceramic piezoelectric drive element is connected to the bearings by flexures in the form of flat washers. The bearings are vibrated in the axial direction by the ceramic tube operating at the longitudinal mode resonant frequency of the system. Tie bolts are used to keep the ceramic tube under compressive preload throughout the cycle. The transducer system with flexures will have a substantially lower resonant frequency than the ceramic tube alone. If the squeeze motion frequency is too low, the load capacity of the bearing will be reduced. Therefore, design of a transducer drive system with mechanical amplification of the vibration amplitude requires a balance between high amplification factor to increase the motion amplitude and maintain acceptably low transducer stresses and power dissipation while, at the same time, keeping the drive frequency high enough to avoid a loss in load capacity.

[An analytical investigation of the axial excursion transducer with mechanical flexures connecting the bearings and the drive element was performed (Ref. 1). The design data given in Ref. 1 can be used to compute the amplification factor and the ratio of the system resonant frequency to the resonant frequency of the drive element as functions of the design variables of the system. These design data were used in the design of the experimental transducer system and to guide the investigation of the effects of some of the critical design parameters.

## II. SUMMARY OF AXIAL-EXCURSION TRANSDUCER PERFORMANCE

An experimental axial-excursion transducer has produced axial vibrations of each of the bearing cones of up to 700 microinches peak to peak with 80 volts rms drive at 11,100 cps drive frequency. With a 45-degree bearing cone angle, this amounts to about 500 microinches peak-to-peak vibration measured normal to the bearing surface. Power consumption under these conditions was approximately 9 watts. The motion of the piezoelectric drive tube was amplified by the flexure supporting the bearing ring by a factor of as much as 6.0.

The following design criteria for squeeze-film bearings have evolved from theoretical design analysis (Ref. 3) and practical fabrication and design considerations:

- a) The bearing squeeze number  $\frac{12\mu (2\pi f)}{P_a} (l/c)^2$  should be greater than 100 to avoid a deterioration in load capacity (the asymptotic squeeze-film solution applies above this limit).
- b) The sum of the half-wave vibratory excursion and the maximum steady-state eccentricity ratio of the bearing should not exceed 0.9. This means that the minimum instantaneous film thickness should always be greater than 0.1 times bearing the clearance gap. This criterion is imposed to account for reasonable expectations regarding machining tolerances and surface distortion.
- c) Given the limitation expressed in b) above, maximum load capacity can be achieved if the vibration excursion ratio is about 0.5 times the mean bearing gap.

The measured half-wave excursion normal to the bearing surface is  $2.5 \times 10^{-4}$  inches. From c) above, this means a mean normal gap of  $5.0 \times 10^{-4}$  inches. Tolerances on bearing cone straightness, roundness, concentricity and match between male and female cone members should be less than 10 percent of the mean gap or 40 to 50 microinches total. The squeeze number of air at atmosphere pressure with  $5.0 \times 10^{-4}$  inch mean clearance and the resonant frequency of the experimental system (11.1 kc) is about 350 which is well above the limiting value for avoiding a frequency effect on load capacity.

The total cyclic stress excursion at the center plane of the ceramic drive tube is approximately  $1.2 \times 10^3$  lb/in<sup>2</sup> and, because of the tie bolt preload, this is a cyclic variation in compressive stress with no stress reversal.

The quality factor (Q) of the transducer system with 80 volts rms drive, 11,100 cps drive frequency was calculated. A high value of Q is desirable to minimize power dissipation and to keep the electrical field strength needed to obtain the desired crystal strain low. A value of several hundred or higher is considered to be good for this type of application. The calculation was performed using the relationship:

$$Q = 2\pi \frac{\text{energy stored}}{\text{energy dissipated per cycle}}$$

The energy stored is approximately equal to the strain energy at maximum displacement. The energy dissipated per cycle was determined from the measured electrical power input. The value of Q calculated in this way was 330 which is quite satisfactory.



### III. EXPERIMENTAL AXIAL-EXCURSION SQUEEZE-FILM TRANSDUCER APPARATUS

The experimental transducer configuration is illustrated in Fig. 1 and the unit as tested is shown in Fig. 2. The cylindrical bars attached to the bearing cone surface are weights which were added to investigate the effects of bearing mass. The tube coming down from the top of the picture is the fiber optic proximity probe in position to measure bearing motion normal to the surface at the c.g. The design parameters and operating variables of the axial excursion transducer include:

$$\begin{aligned}
 \text{a) } \frac{\text{Mass of the driving element}}{\text{Mass of the bearing}} &= \frac{A_1 \rho_1 \ell}{m_b} \\
 \text{b) } \frac{\text{Stiffness of the driving element}}{\text{Stiffness of the flexure}} &= \frac{A_1 E_1}{K \ell} \\
 \text{c) } \frac{\text{Excursion at the bearing}}{\text{Excursion at the drive element end}} &= \frac{C}{\epsilon_0} \\
 \text{d) } \frac{\text{Resonant frequency of the system}}{\text{Resonant frequency of the drive element alone}} &= \nu
 \end{aligned}$$

Fig. 3, taken from Ref. 1, shows the relationship among these parameters. It was decided to use a 3 inch O.D., 0.375 inch thick ceramic cylinder of 2 inch length. The bearing cones were to have a projected area (axial) of 4.4 in<sup>2</sup> and a cone apex angle of 90 degrees. The mass of the bearing cone with 0.125 thick walls is about  $9.1 \times 10^{-4} \frac{\text{lb-sec}^2}{\text{in.}}$  and the mass ratio ( $\frac{A_1 \rho_1 \ell}{m_b}$ ) is 3.4. The design was aimed at an amplification factor of 7.5. As shown in Fig. 3, this results in a desired stiffness ratio of about 8.2 and a predicted frequency ratio of about 0.38. This should be high enough to give a bearing squeeze number well in excess of 100 so there should be no loss in bearing performance because of the reduced frequency. The flexure stiffness required to obtain a stiffness ratio of 8.2 is about  $5.0 \times 10^6$  lb/in.

The flexure dimensions to obtain the desired stiffness were computed using the formula for a flat washer with fixed edges (Ref. 2). The results were regarded as questionable because the proposed flexure is a very thick washer (thickness is nearly half the washer transverse dimension), the choice of end conditions is doubtful, and because small errors in the machined corner radii could substantially alter the stiffness. For these reasons, measurements of the flexure stiffness were made with the actual machined parts. Because of the high stiffness of the flexure, extremely rigid loading fixtures and precise measurements of very small deflections were required. Load was applied by a hydraulic press through a male cone member matching the bearing cones. A strain-gage cantilever beam was made and attached to the ring which fits over the ceramic tube so that it measured relative axial deflection of the bearing cone at the small diameter end. Thus deflections of the supporting structure had no effect on the results. Essentially linear load-deflection curves were obtained which indicated flexure stiffnesses of  $4.35 \times 10^6$  lb/in. and  $4.7 \times 10^6$  lb/in. for the two rings.

The bearing cone-flexure-mounting rings were machined in one piece from low carbon molybdenum alloy. Mo-alloy was chosen for these parts because of its low coefficient of expansion, high thermal conductivity, and high modulus of elasticity. The low coefficient of expansion closely matches that of the ceramic and high conductivity should improve heat dissipation from the ceramic. The high modulus of elasticity ( $46 \times 10^6$  lb/in) results in a high bearing cone stiffness with low weight. The bearing rings are mounted on the ceramic tube with a very light radial interference and with unfilled epoxy in both circumferential and axial joints. A very stiff connection between the ceramic tube and the bearing rings is required for good mechanical coupling. Compressive preload and epoxy-filled joints were used for this purpose.

A lead zirconate-lead titanate material (Gulton HDT-31) was used for the piezo-electric ceramic tube. This material was selected for its relatively high mechanical Q, high Curie temperature, and high resistance to depolarization under high stress. The centerplane mounting ring is to connect the transducer to the surrounding support structure. It is cemented to the ceramic cylinder with unfilled epoxy and is located at the centerplane because this should be the nodal point for the longitudinal mode resonance. The mounting ring was installed after most of the experiments were completed in order to determine the effect on transducer performance.

Compressive preload is applied by 12 stainless steel thread-rod tie bolts through the clamping rings at the ends of the transducer. The amount of preload was determined by measuring the stretch of the individual tie bolts as the nuts were tightened.

The transducer was driven by a power amplifier which, in turn, was driven by a variable-frequency signal generator. Transducer current was measured by measuring the voltage drop across a 12 ohm series resistor. Drive voltage was measured directly.

Vibratory motion amplitudes were measured by Fotonic Model KD-45 fiber-optic proximity sensors. The calibration factor of the sensor was  $5.7\mu$  in/mv. and its frequency response is flat to about 40 kc. The estimated accuracy of measurement is 5 percent or  $\pm 10\mu$  in, whichever is greater. Small triangular blocks were cemented to the bearing cone surface at a number of points (see Fig. 2). The sides of these blocks served as reference surfaces for measurements of motion in the radial and axial planes. The bearing surface itself was used for measurements in the normal direction.

#### IV. EXPERIMENTAL OPERATION OF THE AXIAL-EXCURSION TRANSDUCER

A series of experiments was performed for the purpose of observing the behavior of the transducer-bearing assembly and to investigate approaches for improving performance.

Before beginning a description of the results, some comment regarding the uniformity and reproducibility of the results is appropriate. A decline in the amplitude of vibration on the order of 10 percent commonly occurred between starting the transducer cold and steady-state operation after several hours at high drive voltage. For this reason, data were generally taken after a warm-up period of operation. The temperature rise of the transducer was quite small - the tube temperature reached 95 to 100 F after several hours at 80 volts drive. Variations in performance between separate runs with seemingly identical conditions were not specifically investigated because it was clear from normal testing that the differences were small - considerably less than the 10 percent shift on warm-up.

##### A. Survey of Transducer Resonant Frequencies

The transducer drive frequency was varied from 5 to 60 kc at constant 40 volt rms drive to identify system resonant frequencies in that range. The results, shown as variations in transducer current with frequency, are given in Fig. 4. By far the strongest resonant frequency, with the lowest transducer impedance, is the hoop mode at just over 15 kc. The axial mode, at which the transducer is operated, is appreciably weaker. Relatively close proximity of the dominant hoop mode resonance to the axial resonance will present difficulties in the design of a self-resonant drive circuit to drive at the axial mode resonance. It may be necessary

to incorporate axial motion measurement instrumentation for feedback control of the drive circuit in order to operate on the axial resonance.

Bearing cone motions were measured at each of the numerous resonant frequencies to identify, at least generally, the mode of the vibration. The weak resonance at 12.5 kc is a bending mode of the bearing cones characterized by very little motion at the large diameter end and hoop mode vibration of increasing amplitude going from the large to the small diameter end. The maximum bearing cone motions, at the small diameter end, are only about 15 percent of the motions at the axial mode resonance, so this resonant frequency has little effect on performance at the axial mode resonance. The higher frequency resonances, above 15 kc, also involve bending of the bearing cones and the motion amplitudes are all very small compared to those at the axial mode. At the hoop-mode, there is very large radial motion at the transducer centerplane and much smaller motion at the ends. Bearing cone motion, measured normal to the surface, is quite small, about 10 percent of the motion at the axial mode resonance.

The axial and hoop mode resonant frequencies of a plain ceramic tube identical to that used in the transducer system were measured and found to be 33,277 and 15,443 cps respectively.

#### B. Characteristic Bearing Cone Motion

Ideally, the bearing cone should vibrate in a purely translational mode in the axial direction so that the normal motion of the bearing surface is identical at all points. In fact, this is difficult to achieve because of the following effects:

- (a) Deflection of the flexure results in a moment at the junction with the bearing cone because of edge restraint imposed on the flexure by the cone. This moment tends to rotate the cone cross-section about the flexure connection point, cyclically opening and closing the cone apex angle.

- (b) Inertia effects acting on the cone tend to bend the cone cross-section around the flexure connection unless the resultant and the flexure-cone reaction force passes through the cone, c.g.

To investigate the mode of the bearing cone motion, measurements were made in the axial, radial and normal planes at three points in one radial plane (O.D., I.D. and at the c.g.) and at four radial planes spaced 90 degrees apart. The measurements consistently indicated a rotation of the cone cross section about the flexure connection - evidently a response to the moment induced by the flexure deflection. This effect is shown in Fig. 5 where the axial and radial motions at the three measurement points in one radial plane are plotted for 40 volts drive and 4,000 lb tie bolt preload. The combination of cone translation and rotation which the measurements appear to reflect is illustrated in Fig. 6. The radial motions of the inner and outer edge are 180 degrees out of phase and there is no radial motion at the c.g. The radial motion at the inner edge and the axial motion are additive in the direction normal to the cone surface, while the radial motion at the outer edge subtracts from the axial motion in the normal direction. Cone rotation also produces a variation in the axial plane motion at the three measurement points which, like the radial motion, adds to the motion in the normal direction at the inner edge and subtracts from it at the outer edge.

The motions in the normal direction as determined by projection of the axial and radial plane measurements are compared with direct measurements at each of the three measurement points. The direct measurements uniformly indicate larger amplitudes than the projected measurements in each case. The reason for this is not clear. It may be that the Fotonic sensor probe tip was not parallel with the surface when axial plane measurements were taken (this would result in reduced sensitivity).

The relative axial and radial components of motion and their direction were essentially independent of drive voltage. Thus, the bearing motion normal to the surface at the c.g. was consistently about 85 percent of the motion on the I.D. and 170 percent of the motion at the O.D. Measurements at different points around the bearing cone circumference indicated virtually identical motion amplitudes and no detectable phase difference.

There was no indication of hoop mode vibrations aside from the cone rotation effect.

The motions of the bearing cones at either end of the transducer were identical within the accuracy of measurement.

Simultaneous measurements of bearing cone motion at the c.g. and transducer motion at the outer face of the clamping ring were made to determine the amplification factor. Fig. 7 shows an example of the results for 40 volts drive with 4,000 lb preload and the midplane suspension ring in place. The measured amplification factor is 4.85 which is well below the predicted value of about 7.5.

The system resonant frequency at 40 volts drive, 4,000 lb preload was 11,114 c.p.s. The calculated resonant frequency of the ceramic tube with the tie bolts and clamping rings, but not the bearing rings, attached is about 27,000 c.p.s. Therefore, the measured system resonant frequency is about 0.41 times the resonant frequency of the driving section alone instead of 0.38 as predicted.

The operating point of the experimental transducer with 4,000 lbs preload, 40 volts drive as determined from the measured performance characteristics is plotted in Fig. 3 for comparison with the predicted operating point based on design characteristics. The comparison suggests that there is a discrepancy between the calculated

and actual values of stiffness ratio ( $\frac{A_1 E_1}{K l}$ ). The measured and theoretical amplification factors would agree, if the stiffness ratio was reduced from 8.2 to 5.2 while maintaining the same value of mass ratio.

The drive element stiffness may be lower than the original calculated value because of increased compliance in the area of the connection between the ceramic tube and the flexure rings. Increased compliance in this region would be expected from the following:

- a) The area of the interface between the end of the ceramic tube and the flexure ring is only about one half of the tube cross-section area. This results in a stress concentration in the tube near the ends and a lower stiffness than would be expected if the interface covered the entire area of the tube end.
- b) The actual contact area within the interface is much lower than the total interfacial area because of surface roughness and non-flatness. This would reduce the stiffness of the interface itself. Compressive preload and use of epoxy in the interface should minimize this effect. For  $\frac{A_1 E_1}{K l} = 5.2$  and  $\frac{A_1 \rho_1}{m_b} = 3.4$ , the predicted frequency ratio is about 0.47 while the measured value is 0.41. However, this ratio is based on a calculated value for the resonant frequency of the drive section which assumes uniform compliance of the ceramic tube and infinite stiffness of the connection interface. The actual drive section resonant frequency should be reduced by these effects and this would give a higher value of frequency ratio - closer to the theoretical value of 0.47.

The experimental data suggest that the drive section stiffness was reduced by a factor of 5.2 / 8.2 or 0.63 because of compliance in the region of the tube-to



flexure ring connection. The longitudinal stiffness of the ceramic tube, from midplane to end, is about  $40 \times 10^6$  lb/in if it is assumed that the stress is uniform throughout the tube. If it is assumed that the effective cross-sectional area of the tube is reduced at the end to the area of the interface with the flexure ring, and that this effect extends in for a distance equal to twice the radial width of the interface, an estimate can be made of the effect of the reduced interfacial area on the tube stiffness. In effect, the tube cross section area is reduced by half for a distance of 0.375 inch out of a total of 1 inch. This would reduce the effective stiffness of the crystal by a factor of 0.73 or 6.7/8.2. In order to achieve the indicated reduction in overall stiffness by the factor of 0.63 because of compliance of the interfacial joint alone, the joint stiffness would have to be about  $68 \times 10^6$  lb/in. These figures are reasonable and they suggest that the indicated reduction in drive element compliance could very well be caused by the effects which were mentioned.

Additional data to support the belief that the actual drive element stiffness was lower than the value used in the design calculations will be brought out in the discussions of the effects of drive voltage and preload on transducer performance.

### C. Effect of Drive Voltage

The motion normal to the surface at the c.g. and the product of drive voltage and transducer current at various values of drive voltage for the system with the mounting ring in place and 5,200 lb preload are shown in Fig. 8. At the longitudinal resonance, the current characteristically leads the voltage by about 25 degrees so the power consumption is about 0.9 times the volts-amps. product. This phase difference is apparently a result of the reactive nature of the acoustic load. The resonant frequency at each drive voltage is also specified.

The electrical impedance of the transducer was nearly constant (about a 20 percent increase as drive voltage went from 40 to 80 volts.). This means that power goes up approximately as the square of drive voltage while the amplitude of the motion is roughly proportional to drive voltage. A transducer power level of about 9 watts for 500 $\mu$  in. peak-to-peak vibration amplitude in the normal direction is reasonable expectation for an axial excursion transducer of this size.

Characteristic curves of vibration amplitude vs. drive frequency for several different drive voltages with 4,000 lbs preload are shown in Fig. 9. The data given in both Figs. 8 and 9 show a lower resonant frequency with increased drive voltage. This may be an indication of a lower drive element stiffness due to increased compliance of the tube-to-flexure ring connections as the fluctuating load amplitudes approach the preload at high drive voltages. To check on this, measurements of the amplification factor were made for different drive voltages with the 5,200 lb preload. At 40 volts drive, the amplification factor was 6.0 and at 100 volts drive it had fallen to 5.5. This supports the belief that compliance of the tube-ring connection is principally responsible for the differences between measured and predicted performances.

#### D. Effect of Preload

The effects of tiebolt preload are apparent in Fig. 10 in which the drive voltage-motion amplitude relationship is shown for different values of preload. The rate of increase in amplitude with voltage is lower when there is no preload. With preload, the motion increases more rapidly with voltage until a point is reached where the dynamic forces approach the preload. The slope of the curve then falls off and approaches that of the curve without preload. Evidently, preload acts to increase the stiffness of the drive section, particularly of the tube-to-ring connection region. The frequency-motion curves become asymmetrical when the half-

wave dynamic loads approach the preload as shown in Fig. 11. This is an indication of non-linear coupling between the transducer and the bearing cone.

Amplification factor and frequency ratio were determined for widely varying amounts of preload. The results are plotted in Fig. 3. Preload obviously has a strong effect on amplification factor and the effect is consistent with an increase in drive element stiffness as preload is increased.

The calculated value of the mass ratio  $\frac{A_1 \rho_1 l}{m_b}$  is 2.7 instead of 3.4 for the case of no preload due to removal of the tie bolts and clamping ring. There was no change in calculated stiffness ratio for the method used which ignores any effects of the tube-ring connection.

It is clearly desirable to operate the axial excursion transducer with substantial compressive preload. The following advantages are realized:

- a) Greater drive element stiffness and better coupling between the drive element and bearing rings result in larger bearing excursion amplitudes with lower power loss for a given excursion, and lower ceramic tube strain for a given bearing excursion (higher amplification factor).
- b) The piezoelectric driver and the connections between the drive tube and the flexure rings are under continuous compressive stress which should improve the integrity of the connection.

For these reasons, a compressive preload on the order of 1,500 lb/in<sup>2</sup> stress in the drive tube (4,650 lb. total on the experimental transducer) or higher is recommended.

#### E. Effects of Bearing Mass

The predicted effects of increasing the bearing mass (Fig. 3) are to increase the

flexure amplification factor and reduce the frequency ratio. In order to investigate experimentally, weights totalling 13.2 gms (about 10 percent of the original bearing mass) were cemented onto the bearing cones. The result was a small increase in amplification factor (from 6.0 to 6.2 for 5,200 lb preload, 40 volts drive) and a reduction in frequency ratio (from 0.40 to 0.38). The changes are small which is consistent with the small mass change involved.

The relationship between drive voltage and bearing excursion amplitude with the added weights is shown in Fig. 12. The excursion amplitude for a given drive voltage is slightly higher than it was for the bearing without added weights (490 $\mu$  in. peak-to-peak for 80 volts drive compared to 470 $\mu$  in. with the plain bearings). There was no measurable difference in power requirement at a given drive voltage as a result of adding the masses to the bearing cones.

Evidently, mass could be added to the bearing cones for the purpose of stiffening them against rotation caused by the flexure moment with comparatively little cost to power consumption or drive frequency. A small increase in bearing excursion amplitude for a given drive voltage would probably be realized.

#### F. Effect of Clamping Ring Mass

Increasing the mass of the tie-bolt clamping rings should reduce the amplification factor but increase the motion of the piezoelectric transducer for a given drive voltage. To determine the net effect, weights of 0.316 lb were added to each clamping ring (original weight 0.447 lb) and measurements of bearing cone motion and power were made. The effects of the added mass were:

- a) Bearing cone motion measured normal to the surface at the c.g. increased by about 10 percent.
- b) Resonant frequency fell by less than 1 percent.
- c) Transducer impedance fell by nearly 30 percent and power consumption rose

proportionately.

While it is possible to obtain a small increase in motion by increasing the clamping ring mass, the consequences of increased crystal strain and substantially higher power consumption make this an undesirable path to follow.

#### G. Effect of Centerplane Mounting Ring

In order to be useful in instrument applications, the axial excursion squeeze-film transducer-bearing assembly must be rigidly positioned with respect to its supporting structure. This must be done without severely restricting the transducer performance or transmitting large dynamic forces to the supporting structure. The centerplane of the transducer tube is a logical place to make the connection because longitudinal motion at this point should be zero. Therefore, a thin annular mounting ring was cemented to the crystal at the centerplane with a one mil thick film of epoxy between ring and crystal. The ring was 0.125 inch thick and the width of the annular section is 0.75 inch.

The mounting ring had very little effect on the performance of the transducer at the axial resonance. The bearing cone motion and power consumption were the same as those measured previously without the mounting ring within the 10 percent range of variation normally caused by temperature effects or other uncontrolled variables. The measured axial motion of the mounting ring was very small - less than  $10\mu$  in. at any point. However, there was considerably more radial motion of the ring-about  $30\mu$  in. at 80 volts drive. This is a matter for concern since it suggests that when the mounting ring is clamped rigidly to a support structure, there will be more restraint imposed on the transducer. Additional work is needed to develop a mounting arrangement which avoids this difficulty. One promising approach is to use a triangular or square mounting frame in place of the circular ring.

This arrangement, illustrated in Fig. 13, would accommodate hoop mode motions of the transducer with rigidly positioned mounting points by flexure of the sides of the frame. The frame would be stiff with respect to a shift in the locus of the axis of the transducer yet flexible enough with respect to hoop mode vibrations of the crystal, which do not entail a shift in the transducer axis, so that there would be little restraint from attachment to a rigid structure.

## V. CONCLUSIONS AND RECOMMENDATIONS

The axial-excursion squeeze-film transducer offers worthwhile advantages over other transducer configurations. Larger bearing surface excursions are possible with reduced cyclic stress amplitude in the piezoelectric drive element and, for a given excursion amplitude, the power dissipated in the system is lower. In the experiments, bearing excursion amplitudes of about  $250\mu$  in. (half-wave amplitude) have been achieved as compared with values of radial excursion (weighted for non-uniformity of the radial excursion with an axial position) of about  $120\mu$  in the free-floating ring configuration where the ring serves as both the bearing and the transducer. This means that the mean bearing gap, and therefore the dimensional tolerances of the components, can be increased by a factor of more than 2. This greater than twofold increase in bearing excursion is obtained with a cyclic unit strain in the piezoelectric driver which is less than half as great as that of the free-floating ring configuration. The free-floating ring configuration consumes about 5 watts power to produce a weighted radial excursion amplitude of  $80\mu$  in. The axial excursion transducer requires less than 1 watt for the same excursion amplitude and about 9 watts for  $250\mu$  in. excursion amplitude. The ceramic drive tube temperature never exceeded 100 F after prolonged operation at high excursion amplitude so cooling does not appear to be a serious problem.

The resonant frequency of the axial-excursion system is lower than that of the free-floating ring transducer, but it is still high enough to give bearing squeeze numbers of several hundred. For squeeze numbers greater than about 100, squeeze frequency has no significant effect on bearing performance.

Conical or spherical bearings can be used with the axial-excursion configuration so load capacity and stiffness in the radial and axial direction can be matched and one drive element provides support in both planes.

Comparisons between theoretical design data and experimental results and independent experimental observations show that compliance in the region of the connection between the ceramic drive tube and the flexure ring can significantly reduce the overall drive section stiffness, and therefore, adversely affects the transducer performance. High compressive preload is very helpful in minimizing the effect because it stiffens the connection.

Measurements with the experimental transducer brought out the fact that the bearing cones did not oscillate as rigid bodies. Instead there was a rotation of the cone cross-section accompanying the oscillation. This is attributed to the fact that the cone restrains the edge of the flexure washer at their juncture and therefore, deflection of the flexure is accompanied by a moment on the cone cross section about the flexure juncture. The effects of cone rotation are to add to the oscillatory motion in the direction normal to the bearing surface at the I.D. of the cone and subtract from it at the O.D. The effect is undesirable since it results in a non-uniform bearing surface excursion within the bearing cone. For this reason, a smaller load can be carried before a limiting instantaneous minimum film thickness is reached at the cone I.D. than would be the case if the bearing cone motion were uniform everywhere.

The most effective action for achieving a more uniform bearing surface motion is probably to stiffen the cone by increasing its thickness, or by adding a cylindrical section extending in from the cone I.D. toward the centerplane of the transducer. The experimental results and theoretical design data indicate that a moderate increase in bearing cone mass, resulting from efforts to stiffen the cone, should



result in slightly higher excursion amplitudes at very little cost to the power dissipation or system resonant frequency.

The overall results are clearly encouraging and further development of the axial-excursion transducer culminating in a prototype support for an actual gyro float is enthusiastically recommended. Before a prototype unit with precision bearing surfaces is fabricated, a non-precision transducer assembly of the same size and with the same choice of design parameters as the tentative prototype unit should be fabricated and tested. This preliminary unit should incorporate changes aimed at improved stiffness of the ceramic-to-flexure ring connection and at improved stiffness of the bearing cones.

LIST OF REFERENCES

1. Chiang, T. and Pan, C.H.T., "Analysis and Design Data for the Axial-Excursion Transducer of Squeeze-Film Bearings", MTI-65TR25.
2. Roark, R.J., "Formulas for Stress and Strain", Third Ed. McGraw-Hill Book Co. Inc., New York.
3. Pan, C.H.T., "Analysis, Design and Prototype Development of Squeeze-Film Bearings for AB-5 Gyro-Phase I., Final Report, Bearing Analysis and Preliminary Design Studies", MTI-64TR66, November 1964.

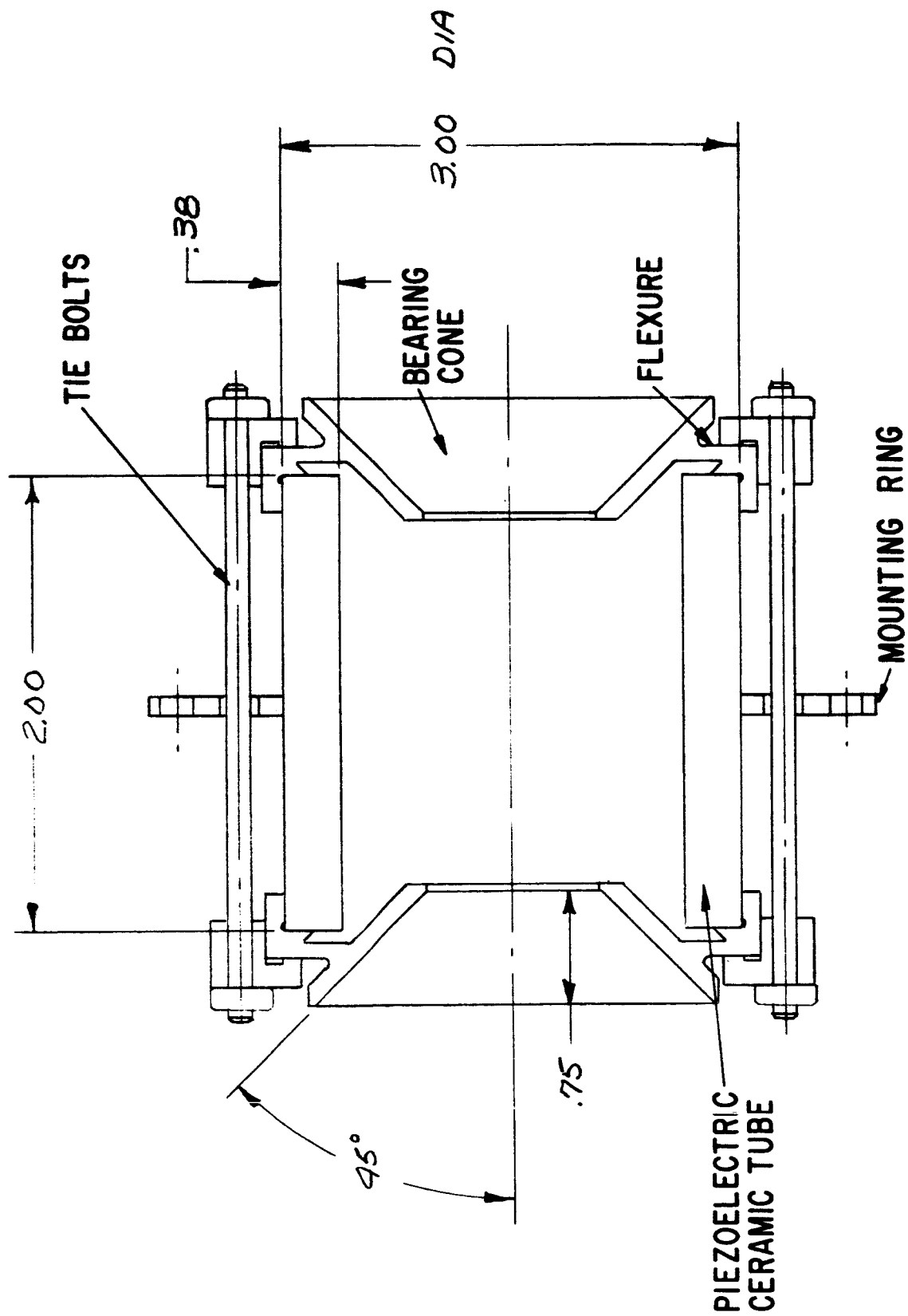


Fig. 1 Experimental Axial-Excursion, Squeeze-Film Transducer Assembly.

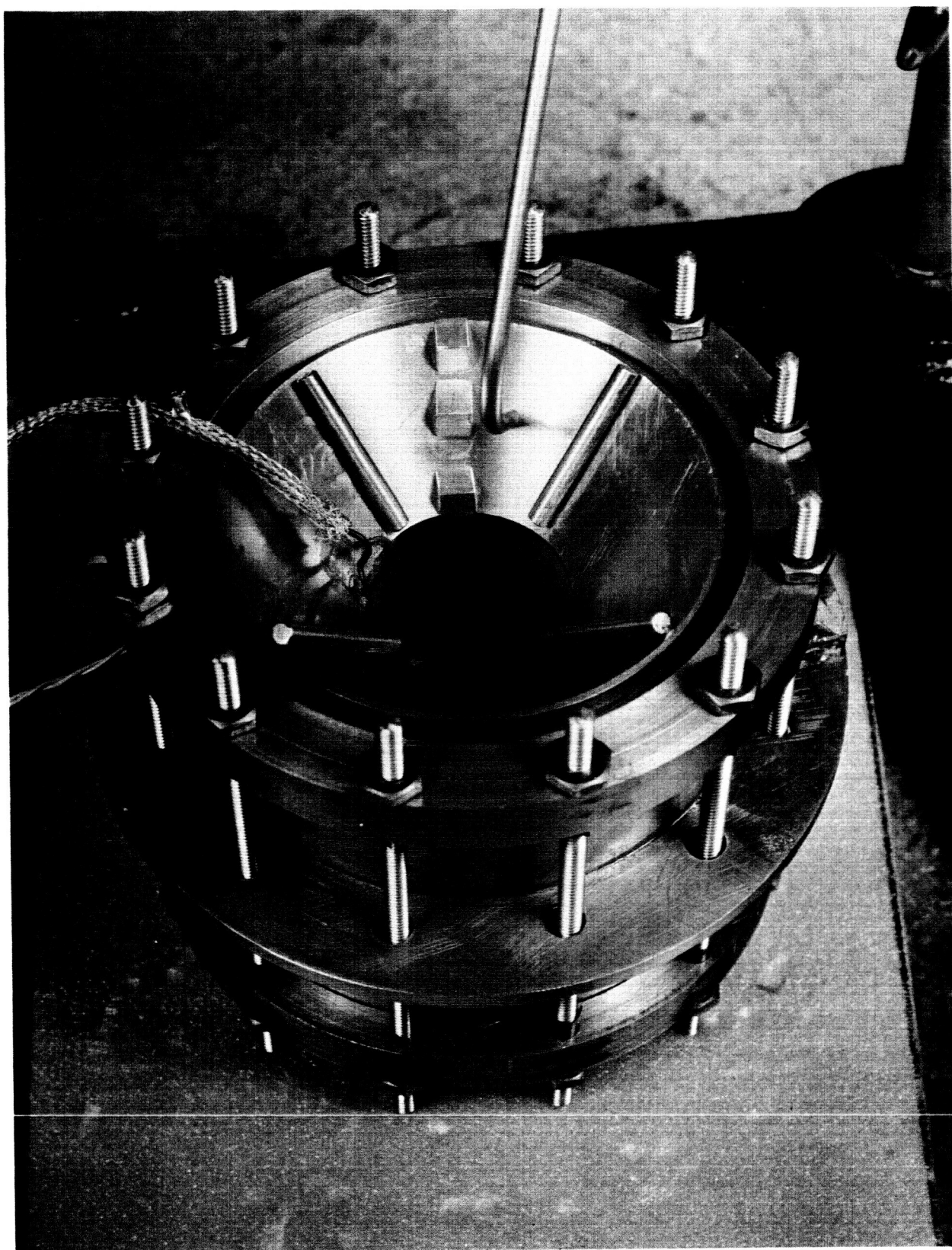


Fig. 2 Non-Precision Experimental Axial-Excursion Squeeze-Film Transducer

- a) The cylindrical bars cemented to the bearing cone are added weights to investigate effects of bearing mass.
- b) A fiber-optic proximity probe is shown in position for measuring normal motion at the e.g.

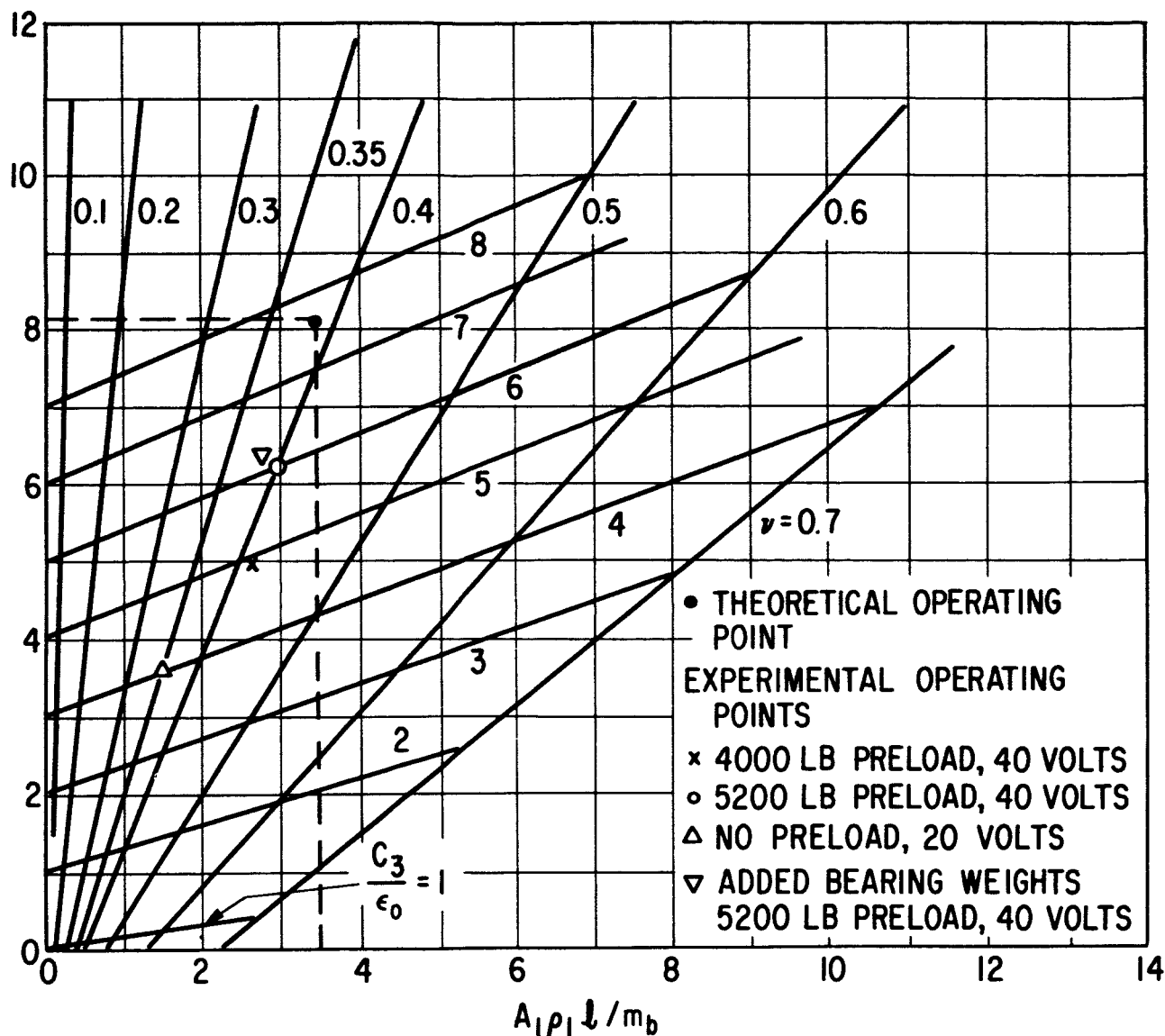


Fig. 3 Stiffness Parameter  $\left(\frac{A_1 E_1}{K l}\right)$  Against Mass Parameter  $\left(\frac{A_1 \rho_1 l}{m_b}\right)$  with Lines Constant Frequency Ratio ( $\nu$ ) and Constant Amplification Ratio ( $C_3/\epsilon_0$ ) (From Ref. 1).

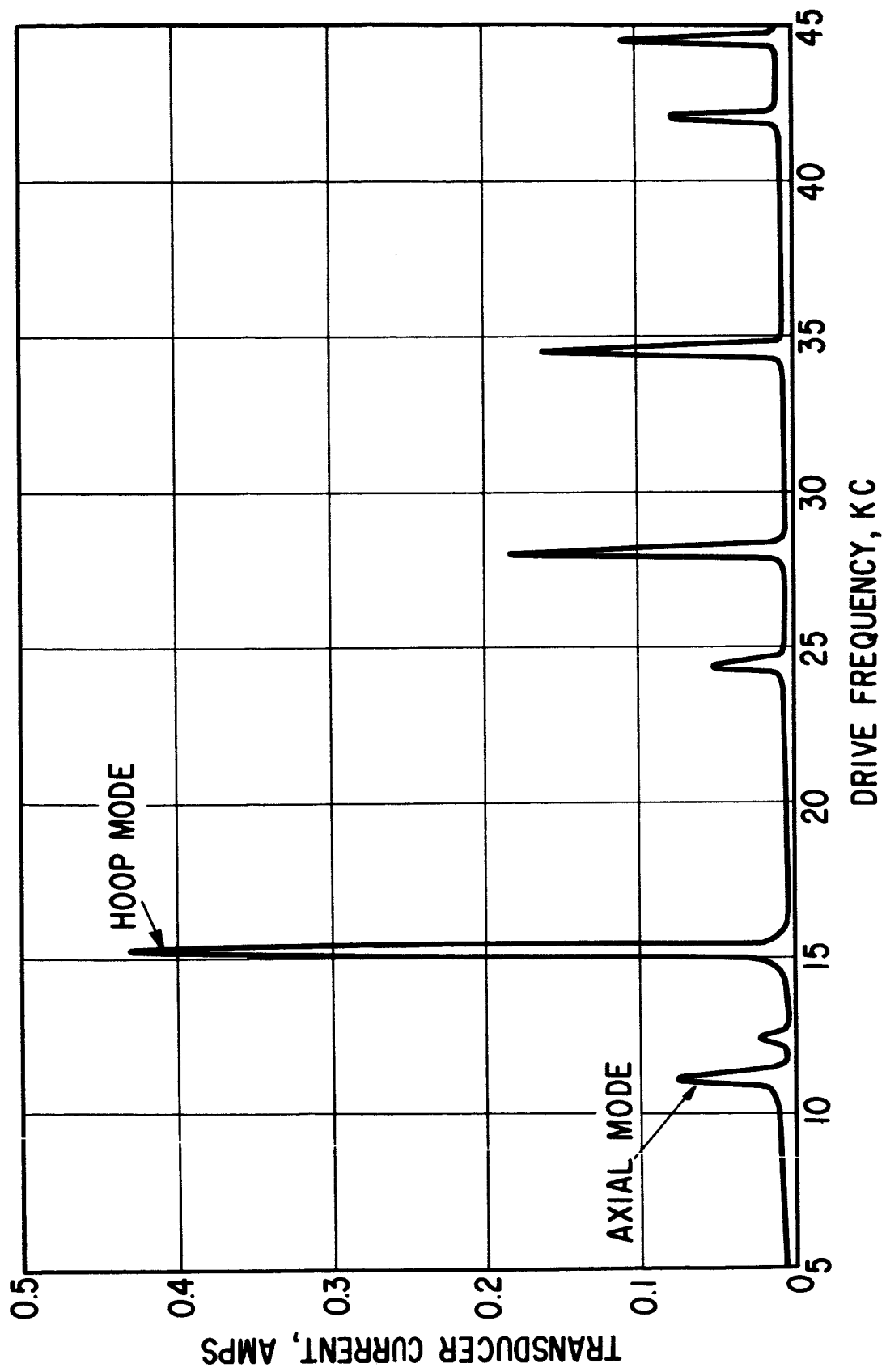


Fig. 4 Transducer Current Over Broad Frequency Range  
40 volts rms drive, 4000 lb preload.

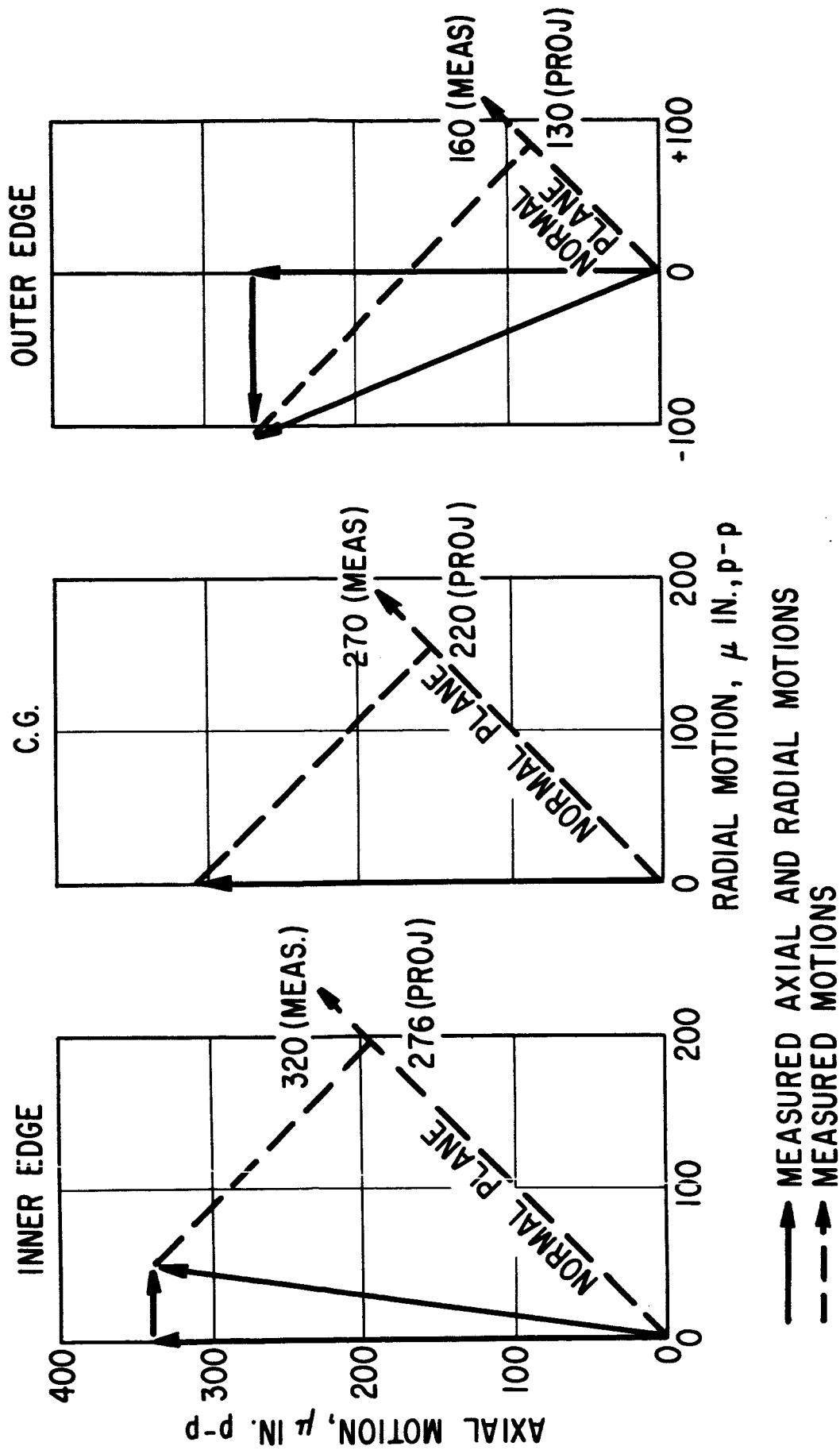


Fig. 5 Bearing Cone Motion Measured at Three Points on One Radial Plane  
40 volts rms drive, 4000 lb preload.

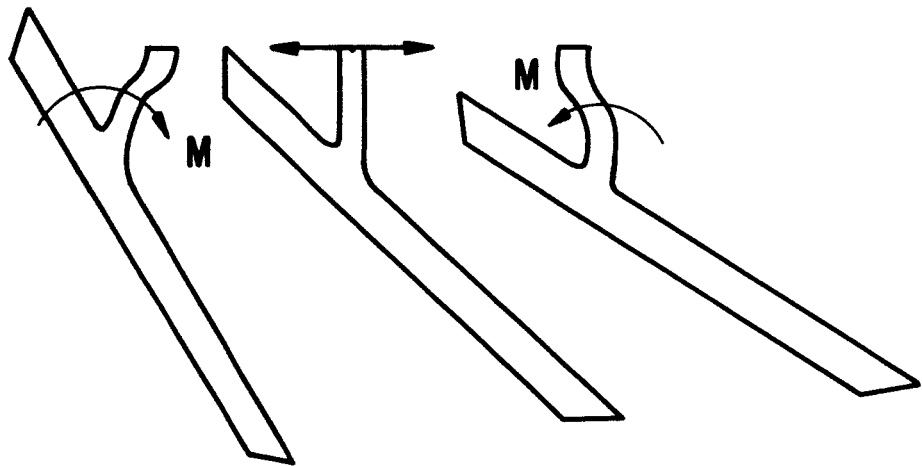


Fig. 6 Illustration of Bearing Cone Motion with Rotation Caused by Flexure End Moment (M).



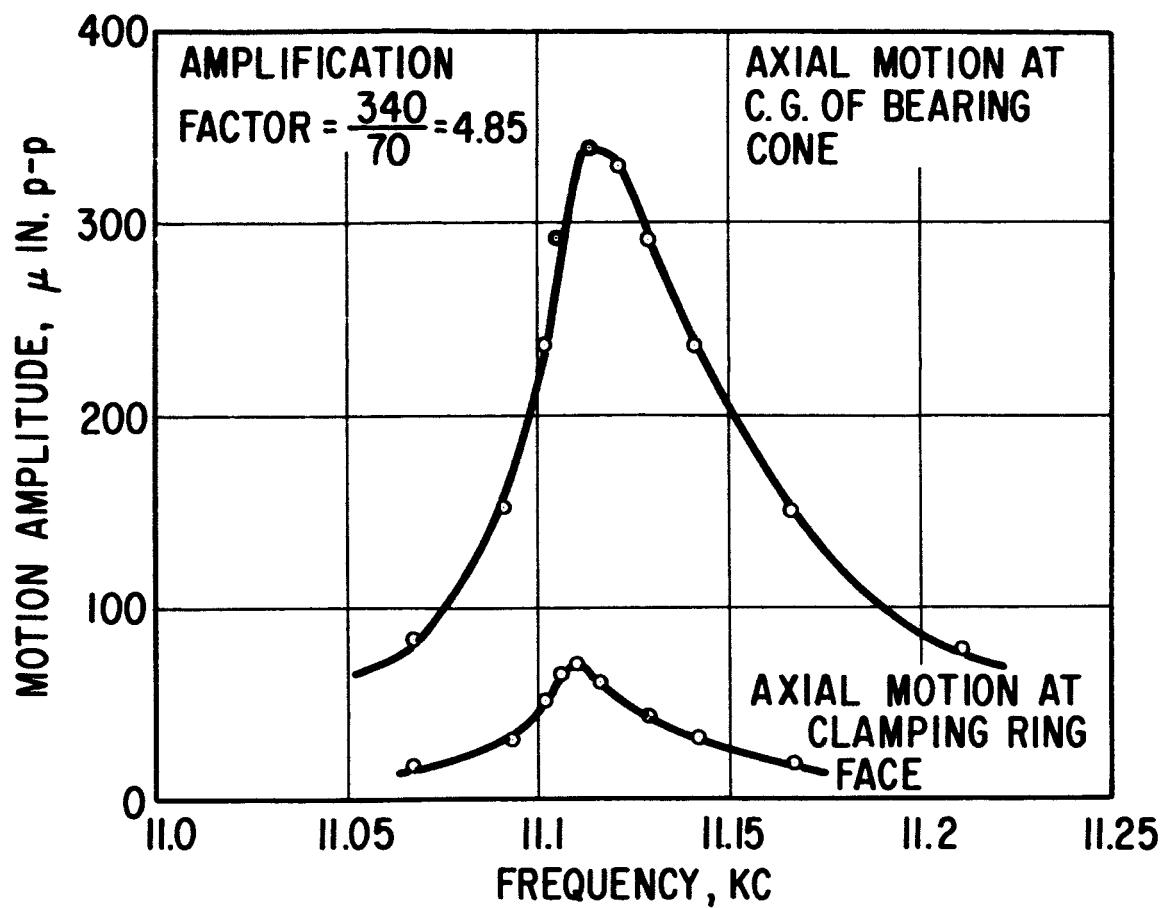


Fig. 7 Comparative Motion at Bearing Cone and Clamping Ring  
 40 volts rms, 4000 lb preload, midplane suspension ring in-place.

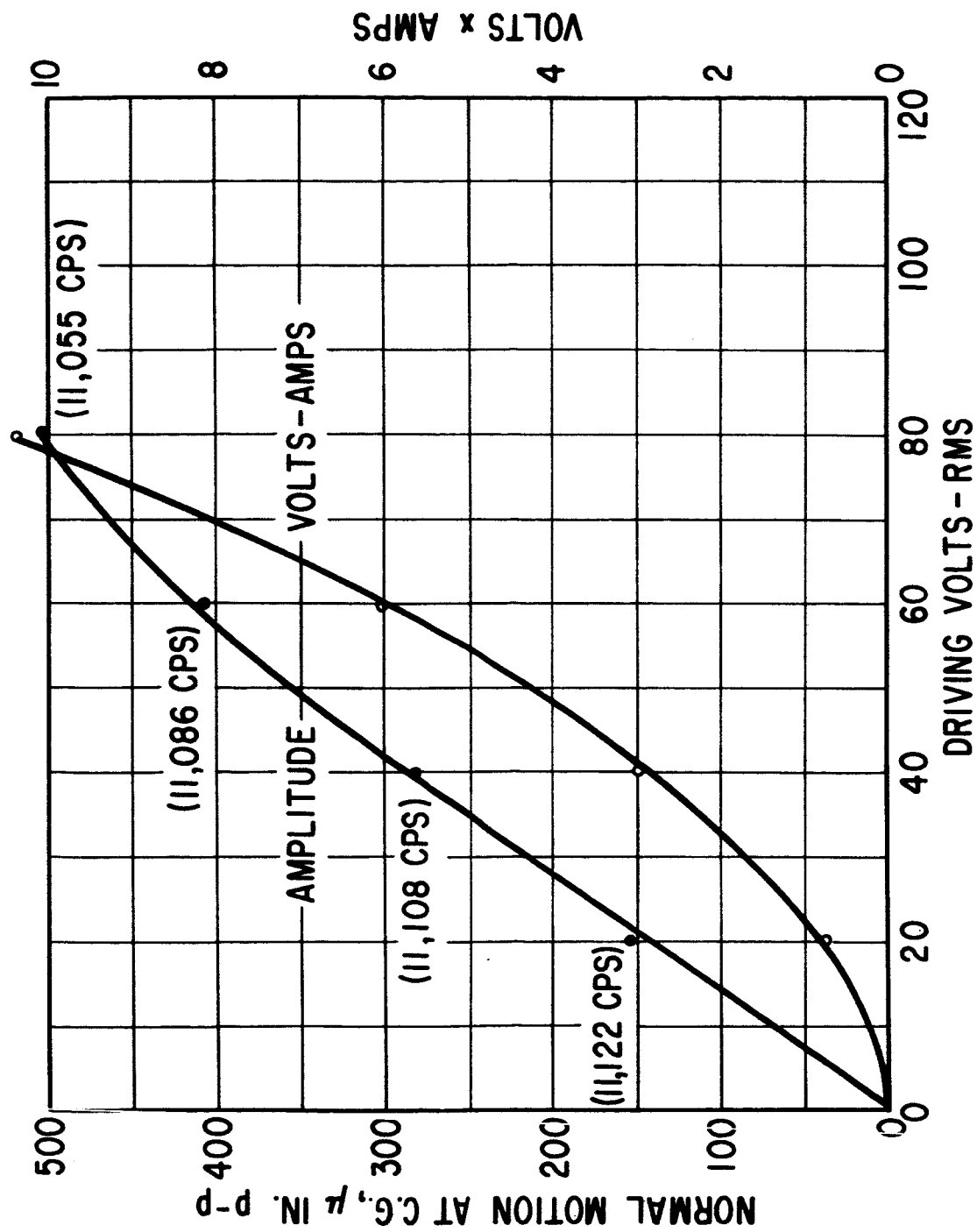


Fig. 8 Bearing Excursion Amplitude and Drive Volts x Amps Product

5200 lb preload, drive power is approximately 0.9 times the volts x amps product. Resonant frequencies at each data point are given in parentheses.

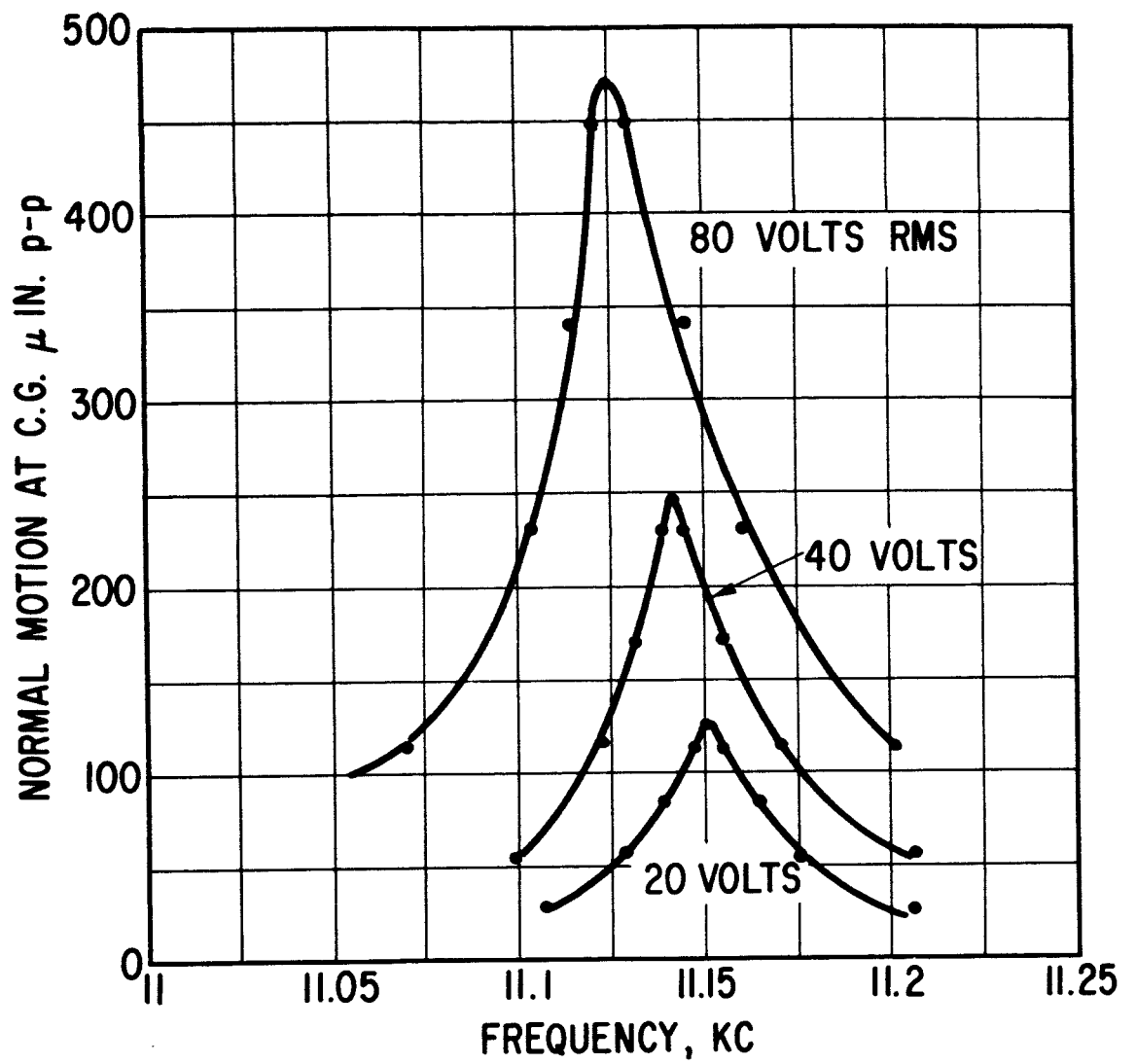


Fig. 9 Motion-Frequency Characteristics for Different Drive Voltages  
4000 lbs preload.

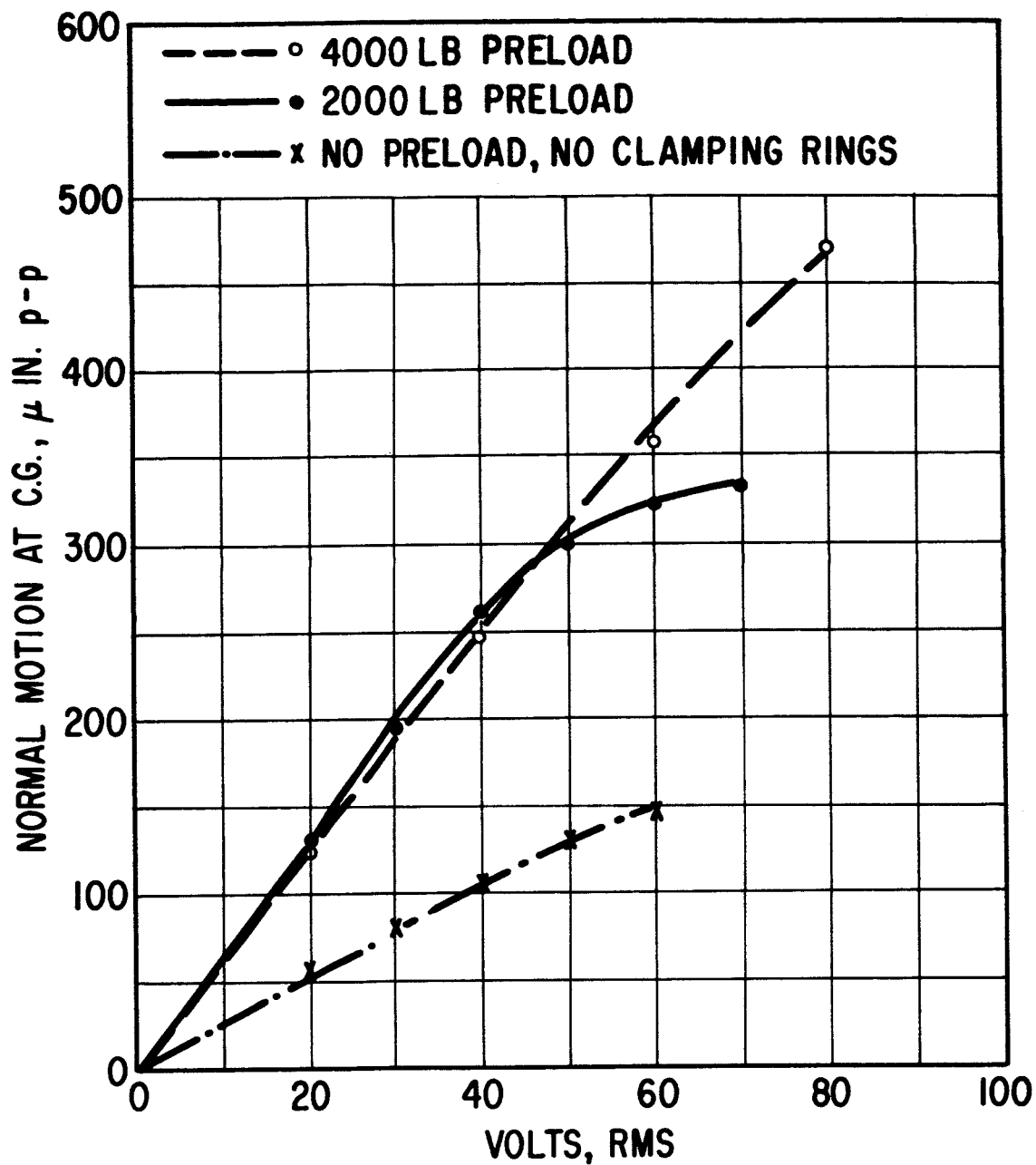


Fig. 10 Voltage-Amplitude Characteristics for Different Preload Conditions  
Centerplane mounting ring removed.

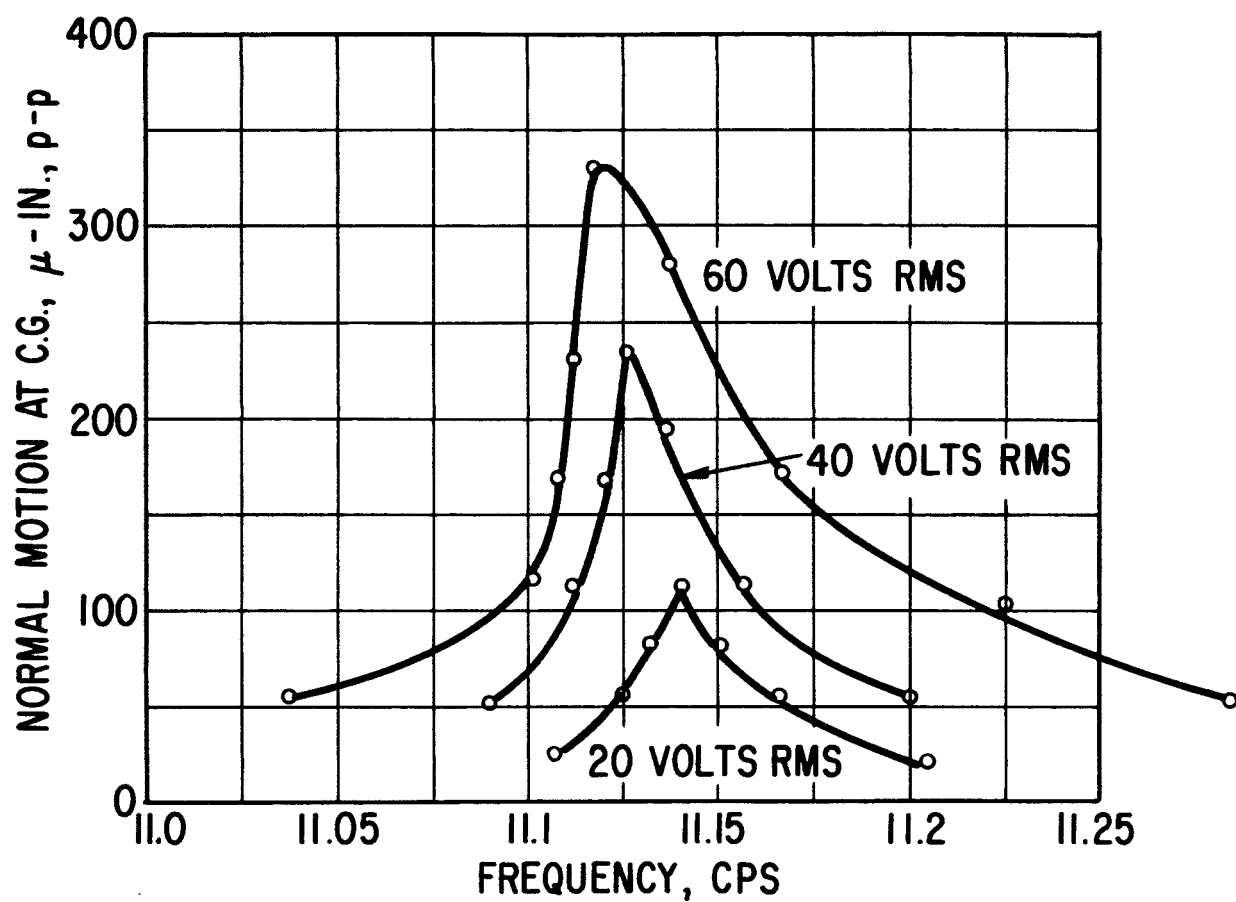


Fig. 11 Motion-Frequency Characteristic for Different Drive Voltages - 2000 lb Preload

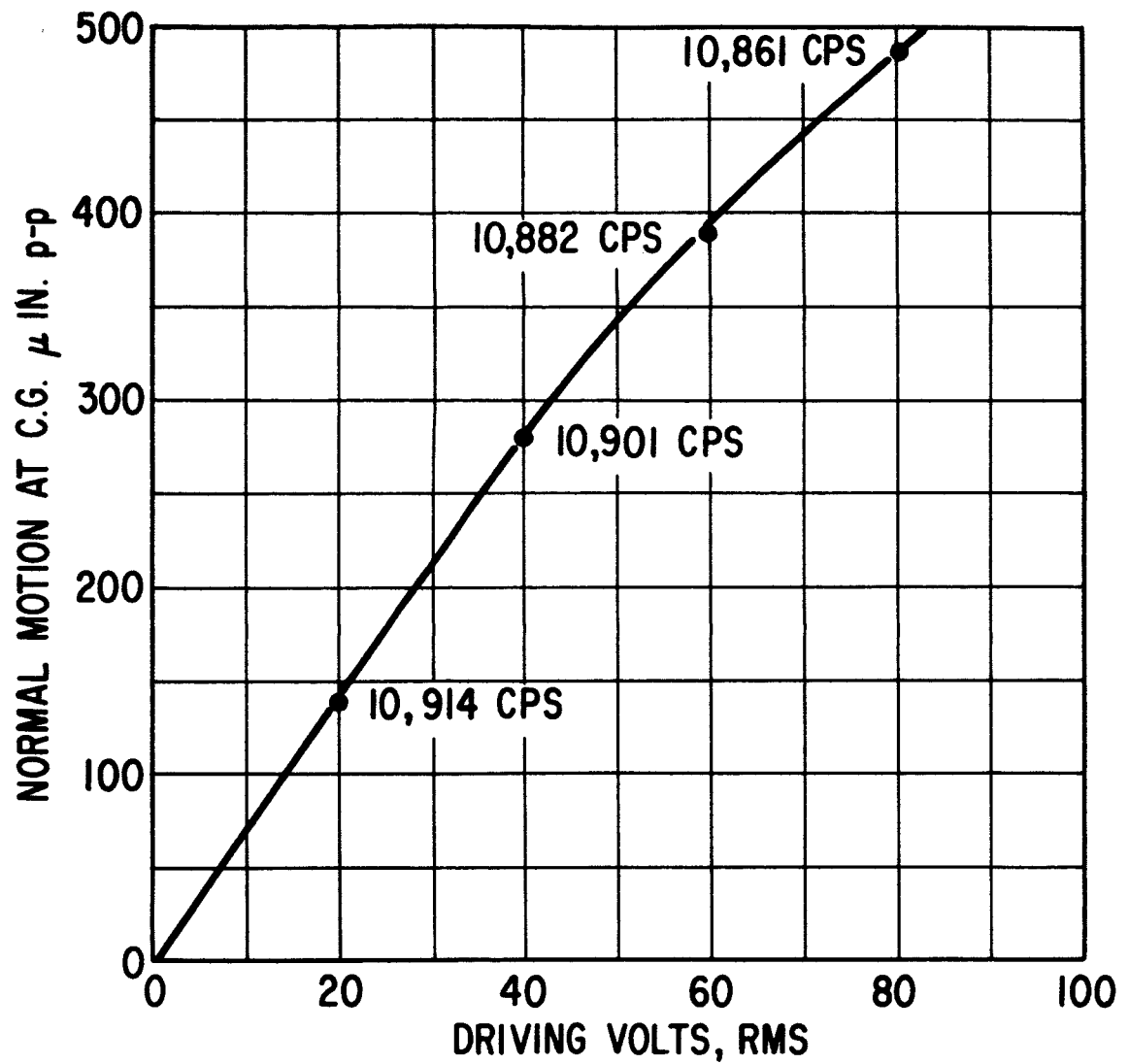


Fig. 12    Excursion Amplitude versus Drive Voltage for Bearing with Added Weights  
5200 lb preload. Resonant frequencies at each data point are given in parentheses.

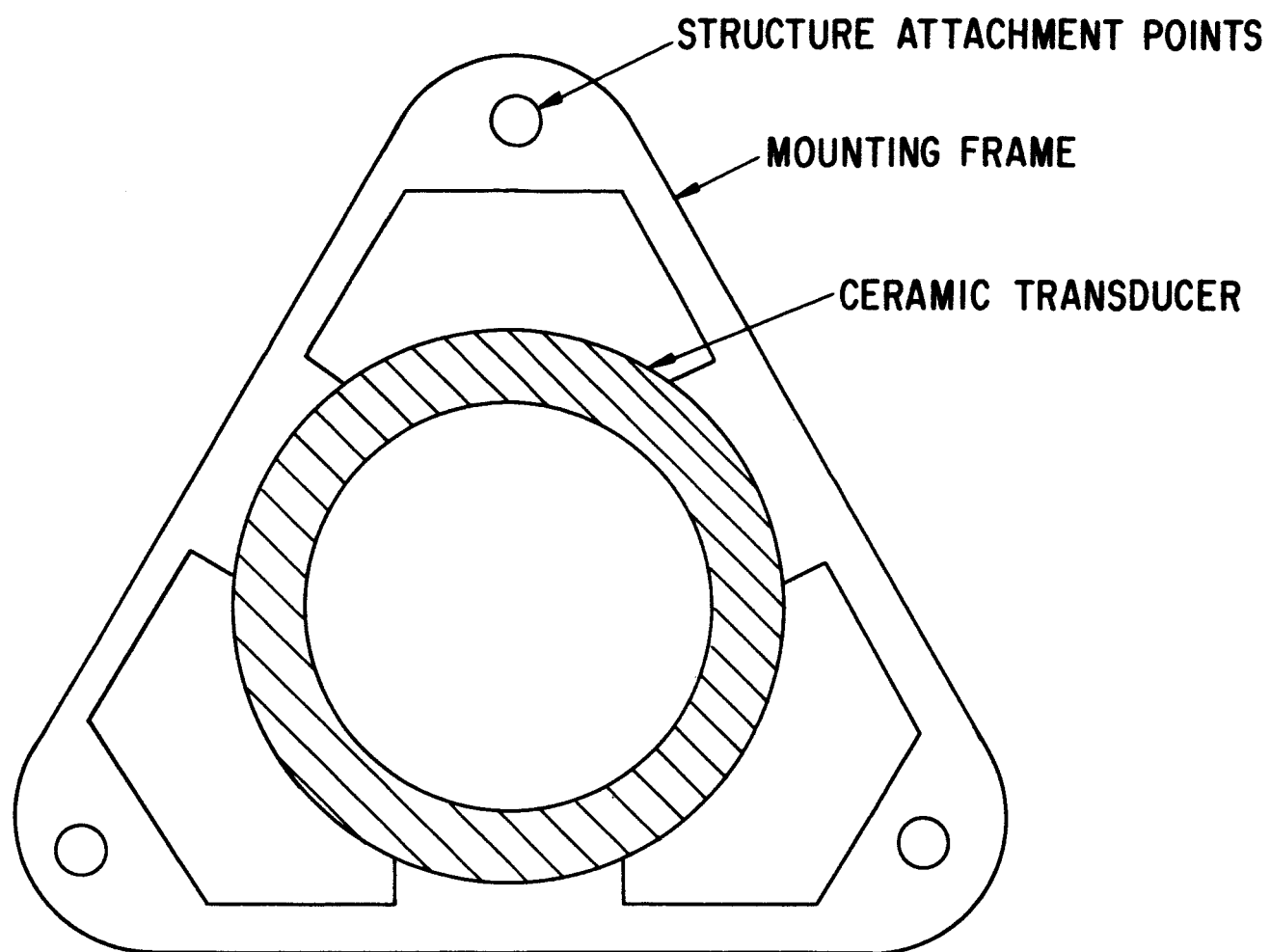


Fig. 13 Flexible-Frame Transducer Mounting Concept